ELSEVIER

Polymer Vol. 37 No. 1, pp. 101–107, 1996

0032-3861/96/$15.00 + 0.00

Permeability and diffusional studies on silicone polymer networks with controlled dangling chains

V. Compañ
Departamento de Física, Universidad Jaume I, Castellón, Spain

and M. A. Villar and E. Vallés
Planta Piloto de Ingeniería Química, CNS-CONICET, Bahía Blanca, Argentina

and E. Riande*
Instituto de Ciencia y Tecnología de Polímeros, CSIC, 28006-Madrid, Spain
(Received 23 November 1994; revised 3 February 1995)

The permeability to oxygen of silicone polymer networks with controlled high-molecular-weight side chains was measured using electrochemical techniques. Networks with controlled amounts of pendent chains were prepared by hydrosilation reactions involving the addition of hydrosilanes from crosslinking molecules to the vinyl end-groups of mono- and difunctional prepolymer molecules. Values of the permeability coefficient P were determined by measuring the steady electric current in an experimental set-up in which several layers of moistened paper were placed between the network and the electrodes. The curve representing the dependence of the permeability coefficient on the molecular weight of the dangling chains, M, shows that, for values of $M < 130\,000$, P is nearly a linear function of M; however, for $M > 130\,000$, the permeability coefficient does not show a noticeable dependence on the molecular weight of the dangling chains. The diffusion coefficient increases with the molecular weight of the side chains, reaching a nearly asymptotic value for $M \approx 170\,000$.

(Keywords: silicone networks; high-*MW* side chains; permeability)

INTRODUCTION

Separation of gas mixtures by means of permeation membranes is a subject of great interest from a technological point of view[1–3]. Most of the membranes used for this purpose are made from glassy polymers, such as polysulfone, cellulose triacetate, polyimides, etc., and, as a common characteristic, all of them present a great selectivity for gases of industrial interest, combined with a low permeability. By greatly reducing the membrane thickness, relatively high fluxes can be achieved through these membranes without losing their selectivity characteristics[4–7].

In general, the diffusional properties of polymer membranes are governed by their chemical structure and morphology. Amorphous polymers with bulky and polar side groups exhibit high glass transition temperatures so that they are commonly used in the glassy state. In this case thermodynamic equilibrium is virtually never obtained and, as a consequence, sorption and transport of gas through these membranes are expected to depend on the thermal history of the membranes[8–14]. Moreover, bulkiness of the side groups increases the rigidity of the chains, which, in turn, reduces packing efficiency, this resulting in an increase of both diffusion and solubility coefficient of gases[14].

In contrast, polymers in the rubbery state are similar to liquids, and sorption and transport in membranes made of these materials do not depend on previous thermal or sorption history. In this case, diffusibility may be mainly conditioned by long-range motions of the main chain, so that the presence of bulky side groups, which enhance the transport of gas in the glassy state, may hinder it in the rubbery state[15,16].

Crystalline order decreases both the sorption of gas in the film and its transport through it. This later process may occur in the amorphous phase[17–19] by random molecular jumping between holes created by short-range conformational transitions in the glassy state, or long-range molecular motions in the rubbery state. The dynamics of the molecular chains, which in turn depend on the chemical structure, play a very important role in the permeation and selectivity of polymeric membranes. It is obvious that the lack of a sufficient understanding of the relationship of the chemical structure of polymers and permeability is responsible for the fact that polymer membranes for separation processes are currently being developed by trial and error using some qualitative principles, such as those described above.

Gas permeation studies carried out in a variety of

* To whom correspondence should be addressed

silicone membranes have shown that substitution of increasingly bulkier functional groups in the side and backbone chains of silicone polymers results in a significant decrease of permeability for a given penetrant gas. It is noteworthy to indicate that backbone substitution seems to have a lesser effect in decreasing the gas permeation than similar substitution in the side chains[20]. In order to get a deeper insight into the effect of chemical structure and membrane topology on gas transport through membranes, we study in this work the permeation characteristics of oxygen through model silicone networks with controlled high-molecular-weight side chains. Special emphasis is given to the effect of dangling chain lengths on the gas transport through these networks.

EXPERIMENTAL

Silicone networks with controlled amounts of pendent chains were obtained by hydrosilation reaction, based on the addition of hydrogen silanes from crosslinking molecules to the vinyl end-groups of mono- and difunctional prepolymer molecules[21]. A commercial difunctional prepolymer (D1) (Dow Corning) was used as the main source of elastically active chains and four monofunctional polymers (M1 to M4) with different molecular weights were used to introduce pendent chains into the elastic network. Monofunctional molecules were synthesized by anionic polymerization of hexamethylcyclotrisiloxane using n-butyllithium as initiator, n-hexane as solvent and tetrahydrofuran (THF) as electron donor[22]. Phenyltris(dimethylsiloxy)silane (Petrarch Systems Inc.) was used as crosslinker and a Pt salt as catalyst; the living polymer was terminated with vinyl dimethylchlorosilane (Petrarch Systems Inc.). The results of the molecular characterization of the prepolymers as well as a description of the other reactants used in the crosslinking reactions are shown in *Table 1*.

Prepolymers with crosslinking agents were weighed in order to obtain stoichiometrically balanced mixtures containing 30 wt% of monofunctional chains of different molecular weight. Reactants were mixed with a mechanical stirrer and degassed under vacuum to eliminate bubbles. Then the reactive mixtures were placed in acrylic moulds. Cure or polymerization reactions were carried out in an oven at 40°C under nitrogen atmosphere. After 24 h, when the mixture had reached the maximum extent of reaction attainable, the networks were removed from the moulds. A scheme of the crosslinking reaction representing the formation of a dangling chain is shown in *Figure 1*, where R and R′ represent sequences of repeat units of poly(1,1-dimethylsiloxane) chains, $-Si(CH_3)_2-O-$. As is obvious, the

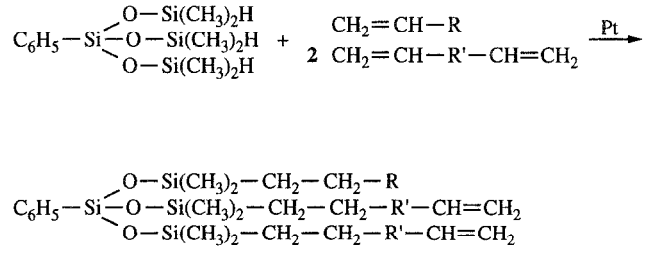

Figure 1 Scheme of the formation of dangling chains in the crosslinking reactions

Table 1 Reactants used in the synthesis of poly(dimethylsiloxane) (PDMS) networks with pendent chains

	M_n		M_w		M_w/M_n
Polymer	*FT*i.r.	G.p.c.	L.a.l.l.s.	G.p.c.	G.p.c.
D1	–	10 800	–	23 900	2.21
M2	21 200	24 200	26 900	26 500	1.08
M3	46 300	47 800	52 400	51 300	1.07
M4	96 600	97 800	128 700	121 300	1.24
M5	–	169 000	–	198 000	1.17

Crosslinking agent (A3)	$[HSi(CH_3)_2O]_3SiC_6H_5$
Catalyst	*cis*-Pt[$(C_2H_5)_2S]_2Cl_2$
D1	Difunctional prepolymer α,ω-PDMS (B2)(including 3.1% of non-reactive polymer)
M_1	Monofunctional prepolymer ω-PDMS (B_1)

Table 2 Summary of the principal characteristics of the networks used

Sample	Monofunctional chains	Stoichiometric imbalance, *r*	Weight fraction of monofunctional chains, w_{B_1}	Weight fraction of solubles
G0	–	1.0002	–	0.0065
G1	M1	1.0508	0.2994	0.0731
G2	M2	1.0558	0.3005	0.0698
G3	M3	1.0004	0.2971	0.0888
G4	M4	1.0351	0.2997	0.1782

Table 3 Calculated molecular structure of the silicone networks with controlled pendent chains

Network	*MW* between crosslinks M_n	M_w	Concentration of active elastic chains, N_u (10^5 mol cm^{-3})
G0	14265	30480	5.64980
G1	23035	47668	1.86020
G2	21799	45246	1.99380
G3	22053	45744	1.81870
G4	31275	63819	0.88423

crosslinking reaction proceeds further by reacting the unsaturated branches with crosslinking molecules.

The weight fraction of solubles was obtained using n-hexane as solvent. Membranes were weighed and placed in Soxhlet extractors in order to remove the uncrosslinked polymer. Samples were then dried under vacuum at 40°C until complete solvent removal was achieved. The dry networks were weighed again and the weight fraction of solubles was calculated. *Table 2* shows the nomenclature and the weight fraction of solubles obtained. The stoichiometric imbalance, r, and the weight fraction of pendent chains, shown in *Table 2*, were calculated by means of the relations:

$$r = \frac{f[A_f]_0}{2[B_2]_0 + [B_1]_0} \tag{1}$$

and

$$w_{B_1} = \frac{m_{B_1}}{m_{A_f} + m_{B_1} + m_{B_2}} \tag{2}$$

where f is the functionality of the crosslinking agent; and $[A_f]_0$, $[B_2]_0$, $[B_1]_0$ and m_{A_f}, m_{B_2}, m_{B_1} are, respectively, the initial concentration in mole and the masses of crosslinking agent (A_f), difunctional prepolymer (B_2) and monofunctional prepolymer (B_1). The concentration of active elastic chains and both number- and weight-average molecular weights between crosslinking points calculated by methods outlined earlier [21] are indicated in *Table 3*.

The experimental set-up for the electrochemical measurements was described in detail elsewhere[16,23]. It consists of a permeometer model 201 T (Rheder Development Co.) in which the polarographic cell is a solid cylindrical cathode of 24 carat gold (4.24 mm in diameter and 6 mm long). The anode is a hollow cylinder made of silver (purity 99.99%), 7 mm long, the inner and outer diameters being 5 and 10 mm, respectively. A thermistor is installed into the anode to monitor the temperature, which was controlled with a precision of 0.1°C by means of a thermostat of water.

ELECTROCHEMISTRY AND OXYGEN PERMEATION: FUNDAMENTAL ASPECTS

Under the driving force of a concentration gradient, oxygen diffuses across the membrane towards the cathode of the polarographic cell. The electrochemical reactions taking place at the electrodes are:

$$O_2 + 2H_2O + 4e^- \rightarrow 4OH^- \quad \text{(cathode)}$$
$$Ag - 4e^- \rightarrow 4Ag^+ \quad \text{(anode)} \tag{3}$$

It is assumed that the diffusion of oxygen occurs in the direction normal to the surface of the membrane, so that the flux of gas can be expressed by Fick's first law:

$$J = -D\frac{\partial C}{\partial x} = -KD\frac{\partial p}{\partial x} \tag{4}$$

where C and p are, respectively, the concentration and partial pressure of oxygen, both quantities at low pressure being related by Henry's law ($C = Kp$); D is the diffusion coefficient, which is assumed to be constant, and the product KD is called the permeability coefficient, P.

The experiments are run under the following conditions:

(a) At the beginning of the experiment, an inert gas, usually nitrogen, is passed through the system in order to eliminate the oxygen present in it. Therefore:

$$p(x = 0, t < 0) = 0 \quad p(x = L, t < 0) = 0 \tag{5}$$

where L is the thickness of the membrane.

(b) The partial pressure of oxygen at the surface of the membrane not facing the cathode ($x = 0$) is kept constant. However, the molecules of oxygen diffusing across the membrane are rapidly reduced once they reach the other side and, as a consequence:

$$p(x = 0, t \geq 0) = p_0 \quad p(x = L, t \geq 0) = 0 \tag{6}$$

Under these conditions and taking into account equation (1), the intensity of current necessary to reduce the oxygen diffusing across the membrane can be written as:

$$I(t) = -nFAJ = nFAKD\left(\frac{\partial p}{\partial x}\right)_{x=L} \tag{7}$$

where n is the number of electrons per unit time transferred from the anode to the cathode to reduce each molecule of oxygen, A is the area of the cathode (= area of the membrane) and F is Faraday's constant. Once steady-state conditions are reached, equation (7) becomes:

$$I(t \rightarrow \infty) = nFADK\frac{\Delta p}{L} \tag{8}$$

where $\Delta p = p_0$.

Under non-steady-state conditions, gas diffusion through the membrane is governed by Fick's second law:

$$\frac{\partial p(x,t)}{\partial t} = D\frac{\partial^2 p(x,t)}{\partial x^2} \tag{9}$$

The analytical solution of this equation in terms of current intensities was performed by Yen and Shih[24–26]. Using the boundary conditions indicated before (equations (5) and (6)), these authors found:

$$\frac{I(\tau)}{I(t \rightarrow \infty)} = 1 - \exp(-6\tau) \tag{10}$$

Where $\tau = Dt/L^2$. Thus from the measurements of $I(t \rightarrow \infty)$ and $I(\tau)$ one can determine the transmissibility (DK/L), and the permeability and diffusion coefficients.

RESULTS

The determination of the permeation characteristics of the silicone networks used in this work was performed by the method described by Fatt[27–29] for the study of the

permeability of hard contact lenses. Modifications suggested by Goldemberg *et al.*[30] have been incorporated with the aim of eliminating non-linear responses occurring in the polarographic cell when the permeability of oxygen through membranes of high permeability is measured.

In order to facilitate the transport of electric current between the cathode and the anode necessary to produce the reduction of oxygen, a piece of moistened absorbent paper was placed between the membrane and the electrodes. In brief, a piece of paper wetted with water and about five drops of borax was placed on the surface of the electrodes. The borax is added to prevent changes in pH, formation of precipitate on the electrodes and the production and decomposition of H_2O_2, which would cause a polarographic overvoltage. Prior to the permeation of oxygen through the moistened paper, the cell was deoxygenated by passing nitrogen through the system. Under constant conditions of humidity and temperature, steady-state current produced by the transport of oxygen was obtained in 20–30 min. Then the membrane under test was positioned over the moistened paper. The vertical hollow cylinder was perfectly adjusted to the membrane and a small quantity of distilled water was introduced by the opening of the cylinder. The system was deoxygenated in a nitrogen atmosphere until the electric current was reduced to zero as a result of the total consumption of oxygen. Oxygen at a pressure of 155 mmHg was bubbled in the water of the hollow cylinder and the transitory that leads to steady-state current was determined. In all the cases, steady-state conditions were obtained in 30–40 min. A further test was done to find out whether the moistened paper had dried during the experiment. For that purpose the membrane was removed, the system deoxygenated and the permeation of oxygen through the piece of paper monitored. Reproducibility of the results to ±2.5% was found in all cases. With the membrane removed, a second piece of moistened paper was placed over the first, proceeding to the determination of the steady-state current. Then the membrane was repositioned on top of the double layer of paper and the steady-state current was obtained in about the same time as in the experiment with a single layer. The experiment was repeated until a total of five pieces of paper were used; in other words, ten experiments (five with membrane and five without membrane) were performed to measure the diffusional characteristics of each silicone network. In all the cases, the dark current or residual current was measured in the deoxygenated system and subtracted from each subsequent current measurement. As an example, the evolution of the net current with time for an experimental assembly with and without membranes is shown in *Figure 2*.

By taking into account that the reciprocal of the transmissibility may be considered as a resistance to gas permeation, the law of resistors in series leads to:

$$\left(\frac{L}{DK}\right)_{\text{app}} = n\left(\frac{L}{DK}\right)_{\text{paper}} + \left(\frac{L}{DK}\right)_{\text{BL}} \tag{11}$$

for the experimental set-up without membrane, and:

$$\left(\frac{L}{DP}\right)_{\text{total app}} = n\left(\frac{L}{DK}\right)_{\text{paper}} + \left(\frac{L}{DK}\right)_{\text{memb}} + \left(\frac{L}{DK}\right)_{\text{BL}} \tag{12}$$

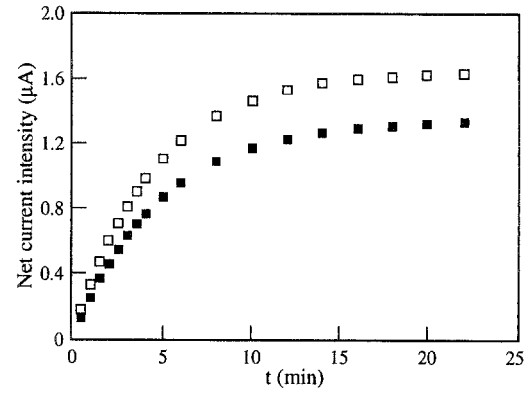

Figure 2 Evolution of the net electric curent intensity for an experimental assembly made up of three moistened paper layers above the G0 (■) and the G4 (□) membranes

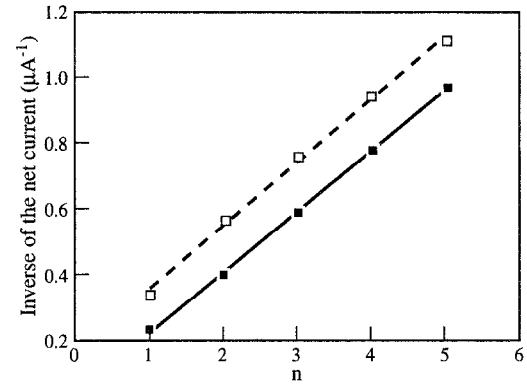

Figure 3 Dependence of the reciprocal of $I(t \rightarrow \infty)$ on the number n of moistened paper layers above the G0 membrane (□) and the same plot for the results with only moistened paper layers in the experimental set-up (■)

for the experimental set-up with membrane. The quantities in parentheses with the subscripts 'paper', 'memb' and 'BL' refer to the transmissibilites of the paper, membrane and boundary layers, respectively.

Transmissibility parameters can be related to current intensity by means of equation (8). This equation leads to:

$$\frac{DK}{L} = \frac{I(t \rightarrow \infty)}{k_c} \tag{13}$$

where $k_c = 1/(nFAp_0) = 0.02826\ (\text{cm}^3\ O_2\ \text{cm})/(\text{cm}^3\ \text{s cmHg}\ A)$. Equations (11) and (12) in combination with equation (13) give:

$$\frac{1}{I_{\text{app}}} = \frac{n}{I_{\text{paper}}} + \frac{1}{I_{\text{BL}}} \tag{14}$$

and

$$\frac{1}{I_{\text{total app}}} = \frac{n}{I_{\text{paper}}} + \frac{1}{I_{\text{memb}}} + \frac{1}{I_{\text{BL}}} \tag{15}$$

By plotting $1/I_{\text{app}}$ against n (equation (14)), and determining the best fit by least-squares analysis, it is possible to extrapolate to zero layers of absorbent paper, thus obtaining $1/I_{\text{BL}}$. Similar plots for the results with the membrane positioned in the experimental set-up (equation (13)) permits one to obtain $1/I_{\text{BL}} + 1/I_{\text{memb}}$. As an example, plots of this kind for the G0 and G2 networks

are shown in *Figures 3* and *4*, respectively. The value of $1/I_{memb}$ obtained by this method, in conjunction with equation (8), allows the evaluation of the transmissibility DK/L. Values of $I(t \rightarrow \infty)$, together with the results for the transmissibility and the permeability coefficient, are given in *Table 4*.

The results for the diffusion coefficient were obtained by the method outlined by Yen and Shih[24]. By writing equation (10) as:

$$\ln\left(\frac{I(t \rightarrow \infty)}{I(t \rightarrow \infty) - I(t)}\right) = \frac{6D}{L^2}t \qquad (16)$$

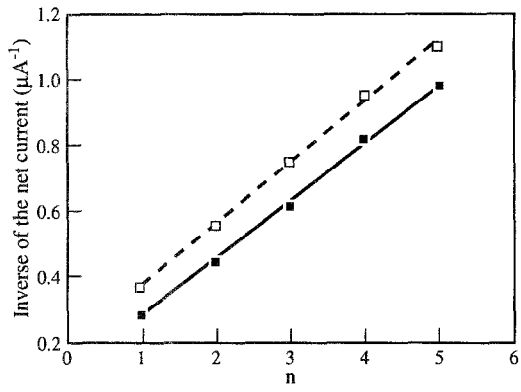

Figure 4 Dependence of the reciprocal of $I(t \rightarrow \infty)$ on the number n of moistened paper layers above the G2 membrane (□) and the same plot for the results with only moistened paper layers in the experimental set-up (■)

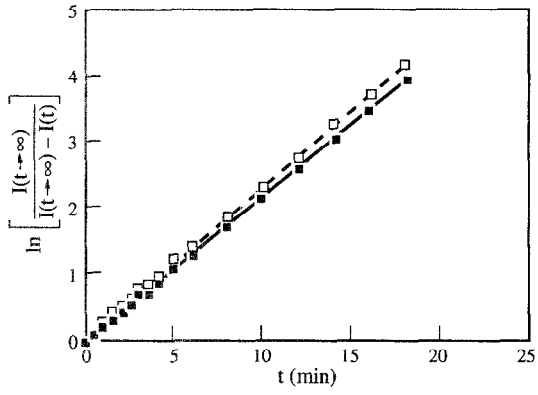

Figure 5 Semilogarithmic plot showing the dependence of $I(t \rightarrow \infty)/[I(t \rightarrow \infty) - I(t)]$ on time for the experimental set-up with three moistened paper layers above the G0 (■) and the G4 (□) membranes

one can obtain the diffusion coefficient from the slope of the semilogarithmic plot of the left-hand side of equation (16) against t. An illustrative plot of this kind is shown in *Figure 5*. Values of this quantity are shown in *Table 4*. Also shown in this table are the values of the solubility coefficient S $(= P/D)$.

DISCUSSION

The gas transport studied in this work occurs through silicone networks with pendent chains, nearly all of them having the same concentration of effective elastic chains, N_u, the only exception being the network with the longest pendent chains, in which the value of N_u is nearly one-half of that found for the other networks. Permeation measurements were also performed on silicone networks without pendent chains (G0) in which N_u is nearly three times larger than that calculated for G1, G2 and G3 networks (see *Table 3*). Owing to the fact that the glass transition temperature of poly(1,1-dimethylsiloxane) lies in the vicinity of −120°C, gas diffusion occurs through the networks in the rubbery state. The free volume will not be a critical parameter for gas transport in this state, as it is when the transport proceeds at temperatures a few degrees above the glass transition temperature, T_g, or below T_g, in the glassy state. In the rubbery state, big changes in the oscillating modes with increasing temperature take place, thus facilitating the jumping of a penetrant molecule through the matrix. Introduction of bulky functional groups either in the side chains or in the backbone will hinder short-range molecular transitions and, consequently, these groups will diminish overall chain mobility, thus reducing the gas transport through the membranes. It is obvious that reduction in chain mobility will be more effective if the bulky groups are located in the side chains than in the backbone; hence the diffusion coefficient should be larger in the former case than in the latter, in agreement with the results reported for the transport of gases through silicone membranes with bulky functional groups incorporated in their structure[20]. As occurs with other transport properties well above the glass transition temperature, Arrhenius behaviour is expected for the diffusion coefficient through the silicone networks.

Reduction of chain mobility can also be achieved by crosslinking well characterized chains, containing reactive end-groups, with a suitable crosslinking agent of functionality three or higher. Polymer networks, prepared by this method, exhibit elastic properties that are strongly dependent on the number of effective elastic chains. The larger the number of these chains, the larger

Table 4 Steady-state current intensity I, transmissibility DK/L, permeability coefficient P, diffusion coefficient D and solubility coefficient S for silicone networks with dangling chains

Network	I_∞ (μA)	DK/L (units[a])	P (barrer)[b]	D (10^6 cm^2 s^{-1})	$S = P/D$
G0	7.60	0.21	273	10.1	27.0
G1	8.85	0.25	322	10.9	29.5
G2	10.50	0.30	450	11.4	39.5
G3	11.20	0.32	458	12.3	37.2
G4	11.90	0.34	471	12.6	37.4

[a] Units: 10^6 cm^2 O_2 cm/(cm^2 s cmHg)
[b] 1 barrer = 10^{-10} cm^3 O_2 cm/(cm^3 s cmHg)

is the modulus of the networks. The perfection of the networks is related to the fraction of solubles they have in such a way that, for a perfect network, this quantity should be zero. However, this never happens; in fact, model networks have a rather complicated topology in which crosslinking points with functionality similar to that of the crosslinking agent can coexist with others of lower functionality. As a consequence, the molecular weight between crosslinking points, M_c, may be somewhat larger than those of the uncrosslinked polymer, and even dangling chains may be present whose mobility is higher than that of the effective elastic chains.

Because of the reduction in chain mobility that crosslinking points impose in the polymer chains, the trifunctional network used in this study, G0, in whose preparation monofunctional prepolymers were not used, exhibits a permeability coefficient significantly lower than that of uncrosslinked poly(1,1-dimethylsiloxane) membranes. Permeation measurements of oxygen through these latter membranes have a value of nearly 1000 barrers at 35°C[20]. This value at 25°C amounts to 254 barrers for the G0 network. By assuming that the activation energy for the diffusion of oxygen through the networks is about 4 kcal mol^{-1}, one finds the value $P \approx 316$ barrers at 35°C, a value that is much smaller than that reported for uncrosslinked PDMS membranes. The presence of dangling chains (networks G1–G4) reduces the number of effective elastic chains and, consequently, both the looseness of the networks and the permeability coefficient increase. Moreover, as the length of the pendent chains increases, the concentration of dangling chains between effective crosslinking points decreases, thus favouring the looseness of the networks and hence the increase of gas permeability. This is confirmed by the experimental results shown in *Figure 6*, where both the permeability and the diffusion coefficients are plotted against the weight-average molecular weight of the dangling chains. The curve representing the permeability coefficient presents two well differentiated regions: For dangling chains with molecular weight below ca. 130 000, the permeability coefficient shows a nearly linear dependence on molecular weight of these chains. However, above this molecular weight, the permeability does not show a noticeable dependence on the dangling chain length.

The diffusion coefficient also increases with the length of the pendent chains, reaching an asymptotic value for molecular weights of about 169 000. Gas transport through membranes involves solution of the gas on the membrane surface and further diffusion of the gas across the membrane. It is expected that the solubility coefficient S ($= P/D$) increases with the looseness of the networks, and hence the increase in permeability observed in the first region of *Figure 6* arises not only from the parallel increase observed in the diffusion coefficient but also from the rise of the solubility coefficient, as can be seen in *Table 4*, where the values of the solubility of oxygen in the networks are given.

CONCLUSIONS

Electrochemical techniques are useful experimental methods to obtain accurate measurements of both the permeability and diffusion coefficients of oxygen through silicone networks.

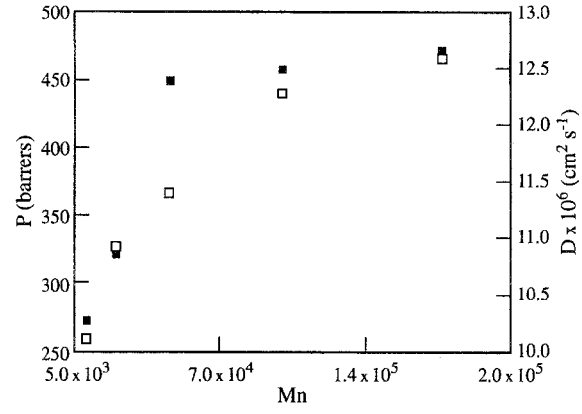

Figure 6 Plots showing the dependence of the permeability coefficient P (■) and the diffusion coefficient D (□) on the molecular weight of the dangling chains

This study suggests that reduction in chain mobility by the effect of crosslinking decreases the diffusional characteristics of the membranes. Though dangling chains increase the oxygen permeability, this effect remains nearly constant above a critical molecular weight, the value of which presumably depends on the topology of the networks.

REFERENCES

1 Stern, S. A. in 'Membrane Separation Processes' (Ed. P. Meares), Elsevier Scientific, New York, 1976
2 Matson, S. L., Lopez, J. and Quinn, J. A. *Chem. Eng. Sci.* 1983, **38**, 503
3 Stern, S. A. in 'Synthetic Membranes' (Ed. M. B. Chenowet), MMI Symp. Ser., Vol. 5, Harwood Academic, New York, 1986, pp. 1–37
4 Strathmann, H. 'Trennung vom Molekularen Mischungen mit Hilfe Synthetischer Membranen', Steinkopff Verlag, Darmstadt, 1979
5 Aptel, P. *Inf. Chim.* 1981, **213**, 189
6 Pusch, W. *Angew.Chem.* 1982, **21**, 660
7 Sykes, G. F. and St Clair, A. K. *J. Appl. Polym. Sci.* 1986, **32**, 3725
8 Kim, T. H., Koros, W. J., Husk, G. R. and O'Brien, K. C. *J. Membr. Sci.* 1988, **37**, 45
9 Kim, T. H., Koros, W. J. and Husk, G. R. *Sep. Sci. Technol.* 1988, **23**, 1611
10 Stern, S. A., Mi, Y., Yamamoto, H. and St Clair, A. K. *J. Polym Sci., Polym. Phys. Edn.* 1989, **27**, 1887
11 Hoehn, H. H. in 'Material Science of Synthetic Membranes' (Ed. D. R. Lloyd), ACS Symp. Ser., No. 269, American Chemical Society, Washington, DC, 1985, p. 81
12 Tanaka, K., Kita, H., Okamoto, K., Nakamura, A. and Kusuki, Y. *Polym. J.* 1990, **22**, 381
13 Tanaka, K., Kita, H., Okano, M. and Okamoto, K. *Polymer* 1992, **33**, 585
14 Tanaka, K., Okano, M., Toshina, H., Kita, H. and Okamoto, K. *J. Polym. Sci., Polym. Phys. Edn.* 1992, **30**, 907
15 Sonnenburg, J., Gao, G. J. and Weiner, H. *Macromolecules* 1990, **23**, 4653
16 Compañ, V., Riande, E., San Román, J. and Díaz-Calleja, R. *Polymer* 1993, **34**, 3843
17 Michaels, S. A. and Bixler, H. J. *J. Polym. Sci.* 1959, **41**, 53
18 Michaels, S. A. and Bixler, H. J. *J. Polym. Sci.* 1960, **50**, 393
19 Holden, P. S., Orchard, G. A. J. and Ward, I. M. *J. Polym. Sci., Polym. Phys. Edn.* 1985, **23**, 709
20 Stern, S. A., Shah, V. M. and Hardy, B. J. *J. Polym. Sci., Polym. Phys. Edn.* 1987, **25**, 1263
21 Vallés, E. M. and Macosco, C. W. *Macromolecules* 1979, **12**, 673
22 Villar, M. A., Bibbó, M. A. and Vallés, E. M. *J. Macromol. Sci.-Pure Appl. Chem. (A)* 1992, **29**, 391

23 Compañ, V., Garrido, J., Manzanares, J. A., Andrés, J., Esteve, J. S. and López, M. L. *J. Optom. Vis. Sci.* 1992, **69,** 685
24 Yen, S. K. and Shih, H. C. *Clin. Exp. Optom.* 1988, **135,** 1169
25 Kimble, M. C., White, R. E., Tsou, Y.-M. and Beaver, R. N. *J. Electrochem. Soc.* 1990, **137,** 2510
26 Linek, V., Benes, P. and Vacek, V. *J. Electroanal. Chem.* 1984, **169,** 223
27 Fatt, I. *Int. Cot. Lens Clin.* 1984, **11,** 175
28 Brennan, N. A., Efron, N. and Holden, B. A. *Clin. Exp. Optom.* 1986, **69,** 82
29 Brennan, N. A., Efron, N., Holden, B. A. and Fatt, I. *Ophth. Phys. Opt.* 1987, **7,** 485
30 Goldemberg, M. S., Rennwantz, E. and Beckman, A. *Int. Clin. Lens Cont.* 1991, **18,** 154